An Automated Method to Parameterize Segmentation Scale by Enhancing Intrasegment Homogeneity and Intersegment Heterogeneity

ARTICLE *in* IEEE GEOSCIENCE AND REMOTE SENSING LETTERS · FEBRUARY 2015

Impact Factor: 2.1 · DOI: 10.1109/LGRS.2015.2393255

3 AUTHORS:

Jian Yang
University of Toronto
7 PUBLICATIONS **5** CITATIONS
SEE PROFILE

Yuhong He
University of Toronto
36 PUBLICATIONS **188** CITATIONS
SEE PROFILE

Qihao Weng
Indiana State University
111 PUBLICATIONS **4,122** CITATIONS
SEE PROFILE

An Automated Method to Parameterize Segmentation Scale by Enhancing Intrasegment Homogeneity and Intersegment Heterogeneity

Jian Yang, *Student Member, IEEE*, Yuhong He, and Qihao Weng, *Member, IEEE*

***Abstract*—Image segmentation is a key step in geographic object-based image analysis. Numerous segmentation techniques, e.g., watershed segmentation, mean-shift segmentation, and fractal net evolution algorithm, have been proposed and applied for various types of image analysis tasks. The majority of the segmentation algorithms require a user-defined parameter, namely, the scale parameter, to control the sizes of segments, yet the automation of the scale parameter remains a great challenge. Over the past few years, several automated parameterization methods, such as the estimation of scale parameters (ESP) tool, have been developed. However, few of the existing methods are able to enhance both intrasegment homogeneity and intersegment heterogeneity. In this letter, we proposed an energy function method that aimed at enhancing the characteristics of intrasegment homogeneity and intersegment heterogeneity, simultaneously, to identify the optimal segmentation scale for image segmentation. The intersegment heterogeneity was calculated as the weighted gradient from a segment to its neighbors by spectral angle, whereas the intrasegment homogeneity was quantified by the mean spectral angle within a segment. The performance of the proposed method was evaluated by applying it to a WorldView-2 multispectral image of Toronto, Canada, and comparing it with the local-peak-based method, which considered only the intrasegment homogeneity of an image. The scale parameter identified by the proposed method can better characterize the reference geo-objects over the entire image. The accuracy assessment result shows that the proposed method outperformed the existing technique by reducing the discrepancy by 17.9%.**

***Index Terms*—Automated parameterization, geographic object-based image analysis (GEOBIA), image segmentation, urban areas, WorldView-2.**

I. Introduction

GEOGRAPHIC object-based image analysis (GEOBIA) is an emerging and evolving paradigm in the discipline of remote sensing [1]. With the increasing availability of very high spatial resolution images, it has attracted growing attention for many remote sensing applications over the past decade. In the workflow of GEOBIA, image segmentation is commonly believed to be the initial and most important procedure to impact the subsequent processing necessary for image exploitation and interpretation. A myriad of segmentation algorithms have been proposed, such as mean-shift segmentation [1]–[3], fractal net evolution approach [4], [5], and watershed segmentation [6]–[9]. In the aforementioned segmentation methods, the most important user-defined parameter, usually called the scale parameter, is used for controlling the intrasegment homogeneity and the intersegment heterogeneity, as well as the sizes of segments. However, automated optimal scale parameterization is still challenging and problematic due to the complexity of geo-objects.

Presently, only a limited number of studies have developed automated methods for optimal scale parameter selection [10]–[16]. In lieu of the supervised methods, the automated optimal scale parameterization is completely expert knowledge independent without needing to manually digitize reference polygons. Specifically, [15] introduced the average local variance of the geo-objects in all of the layers to measure the intrasegment homogeneity and to stop the iterations at the best scale parameter by implementing a three-level hierarchy concept. Moreover, [16] proposed a multiband approach to select the appropriate scale parameters for multiscale image segmentation. The spectral angle was calculated for quantifying intrasegment homogeneity, and multiple appropriate scale parameters were identified based on the magnitudes of local peaks (LPs) in the curve of the derivative of global mean spectral angle.

Ideally, an optimal scale parameter is able to simultaneously enhance intrasegment homogeneity and intersegment heterogeneity for the entire image. Although [15] and [16] were able to make full use of multiple spectral bands, these methods ignored the importance of intersegment heterogeneity. This letter addressed this issue by proposing a new energy function by enhancing intrasegment homogeneity and intersegment heterogeneity simultaneously. Building on the work of [16], this study selected the optimal scale parameter at the largest value of LP index in the curve of the derivative of global energy function, rather than mean spectral angle. In order to demonstrate the importance of intersegment heterogeneity on segmentation scale parameterization, the segmentation results optimized using the proposed energy function were visually and quantitatively compared with those optimized using the intrasegment homogeneity. The remainder of this letter is organized as follows. In the second section, details of the developed method for optimal scale parameter selection are described. The third and fourth sections demonstrate the comparative results and discussion, respectively. The main conclusions are drawn in the last section.

Manuscript received November 22, 2014; revised December 24, 2014; accepted January 14, 2015.

J. Yang and Y. He are with the Department of Geography, University of Toronto, Toronto, ON M5S 3G3, Canada, and also with the Department of Geography, University of Toronto Mississauga, Mississauga, ON L5L 1C6, Canada (e-mail: jiangeo.yang@mail.utoronto.ca; yuhong.he@utoronto.ca).

Q. Weng is with the Center for Urban and Environmental Change, Department of Earth and Environmental Systems, Indiana State University, Terre Haute, IN 47809 USA (e-mail: qweng@indstate.edu).

Color versions of one or more of the figures in this paper are available online at http://ieeexplore.ieee.org.

Digital Object Identifier 10.1109/LGRS.2015.2393255

II. METHODS

Here, we first introduced an energy function for quantifying both intrasegment homogeneity and intersegment heterogeneity. The LP-based method [16] was thereafter applied to the energy function and further used to select the optimal scale parameter. At the end, we modified the previously proposed discrepancy measure i.e., (Euclidean Distance 3, (ED3) [16]) for segmentation evaluation.

A. Energy Function for Enhancing Intrasegment Homogeneity and Intersegment Heterogeneity

It was validated by [16] that the multiband-based metric (i.e., mean spectral angle) was more effective to measure intrasegment homogeneity than the single-band based metric (i.e., standard deviation). Specifically, the mean spectral angle of a segment θ_{MEAN} was defined by the expression given in

$$\theta_{\mathrm{MEAN}} = \frac{1}{I}\sum_{a,b\in P}\cos^{-1}\left(\frac{\sum_{j=1}^{J} a_j b_j}{\sqrt{\sum_{j=1}^{J} a_j^2 \sum_{j=1}^{J} b_j^2}}\right) \tag{1}$$

where a and b are any pair of two pixels within a segment; J is the number of spectral bands; and a_j and b_j are the reflectance spectra component j of a and b, respectively. P is the set of all the pairs of two pixels in this segment, and I is the number of elements in the set P. Moreover, the global indicator of intrasegment homogeneity Θ_{MEAN} was produced by

$$\Theta_{\mathrm{MEAN}} = \frac{1}{\Omega}\sum_{k=1}^{\Omega}\theta_{\mathrm{MEAN}}(k) \tag{2}$$

where $\theta_{\mathrm{MEAN}}(k)$ denotes the mean spectral angle of the segment k, and Ω denotes the number of segments over the entire image.

Intersegment heterogeneity also needs to be taken into account for characterizing the fitness of the segments for matching geo-objects over scale parameter. Thus, an energy function, i.e., e, was designed by this study to achieve the goal that both intrasegment homogeneity and intersegment heterogeneity were simultaneously considered and enhanced, as given by

$$e = \frac{\theta_{\mathrm{MEAN}}}{\sum_{SN\in NSS} w_{SN}\cos^{-1}\left(\frac{\sum_{j=1}^{J}\overline{S_j}\,\overline{SN_j}}{\sqrt{\sum_{j=1}^{J}\overline{S_j}^2\sum_{j=1}^{J}\overline{SN_j}^2}}\right)} \tag{3}$$

where S represents a given segment, whereas SN represents a neighboring segment of S. $\overline{S_j}$ and $\overline{SN_j}$ represent the mean spectra component j within S and SN. NSS represents neighboring segments of S. In particular, w_{SN} is the weight of SN, which impacts intersegment heterogeneity of S and can be derived using

$$w_{SN} = \frac{l_{b(SN)}}{l_{b(S)}} \tag{4}$$

where $l_{b(S)}$ is the boundary length of segment S, and $l_{b(SN)}$ is the common boundary length of S and one of its neighboring segments SN. It can be noted that the numerator of (3) denotes intrasegment homogeneity for S, whereas the denominator is a gradient measure of its neighboring segments to represent intersegment heterogeneity. Since the size of a segment determines the importance over the entire image, this study improved the global indicator, i.e., E, through the consideration of area-based weight, i.e., w, as given by

$$E = \sum_{k=1}^{\Omega} w\cdot e(k) \tag{5}$$

where $e(k)$ is the energy function of the segment k, and w is calculated by the area of segment k divided by the area of entire image.

B. LP-Based Optimal Scale Parameterization

Ideally, the segment boundaries are retained in segmentation at a few subsequent scale parameters when the segments completely match the corresponding geo-objects [13], that is, the boundaries of geo-objects are exactly delineated by the segmentation. At this scale parameter, the tendencies of E and Θ_{MEAN} abruptly become rather flat, which enables the generation of an LP in the curves of the derivatives of E and Θ_{MEAN} over the scale parameter [16]. Thus, the LP was considered as the signal for optimal scale parameterization [16], and the LP magnitude, i.e., I_{LP}, was defined by

$$\begin{aligned} I_{\mathrm{LP}} &= \left(\dot{H}(l)-\dot{H}(l+\Delta l)\right)+\left(\dot{H}(l)-\dot{H}(l-\Delta l)\right) \\ &\quad \dot{H}(l)-\dot{H}(l+\Delta l)>0 \text{ and } \dot{H}(l)-\dot{H}(l-\Delta l)>0 \\ \dot{H}(l) &= \frac{H(l)-H(l-\Delta l)}{\Delta l} \end{aligned} \tag{6}$$

where $H(l)$ denotes the metric of E or Θ_{MEAN} at scale parameter l, and Δl denotes the interval of scale parameter. Specifically, the largest value of I_{LP} represents the optimal scale parameter. In this letter, the proposed energy function E and the mean spectral angle Θ_{MEAN} were adopted for I_{LP} calculation, respectively.

C. Segmentation Evaluation

The quality of segmentation was validated by visual interpretation and discrepancy measurement, of which the latter was proven effective as a quantitative assessment [17]. ED3 was recently proposed by [16] for incorporating geometric and arithmetic discrepancy measures, which outperformed the other new metric [i.e., Euclidean Distance 2 (ED2)] [18]. When a reference polygon corresponds to more than one segment, however, it can contribute more to ED3 than other polygons that only correspond to one segment. In order to ensure the equal weight for all of the reference polygons, we modified ED3 as given by

$$\begin{aligned} \mathrm{ED3}_{\mathrm{Modified}} &= \frac{1}{I}\sum_{i=1}^{I} \\ &\times\left(\frac{1}{J_i}\sum_{j=1}^{J_i}\sqrt{\frac{\left(1-\frac{\mathrm{Area}(r_i\cap s_j)}{\mathrm{Area}(r_i)}\right)^2+\left(1-\frac{\mathrm{Area}(r_i\cap s_j)}{\mathrm{Area}(s_j)}\right)^2}{2}}\right) \end{aligned} \tag{7}$$

where r_i is a reference polygon, and I is the number of reference polygons, whereas s_j is a corresponding segment for

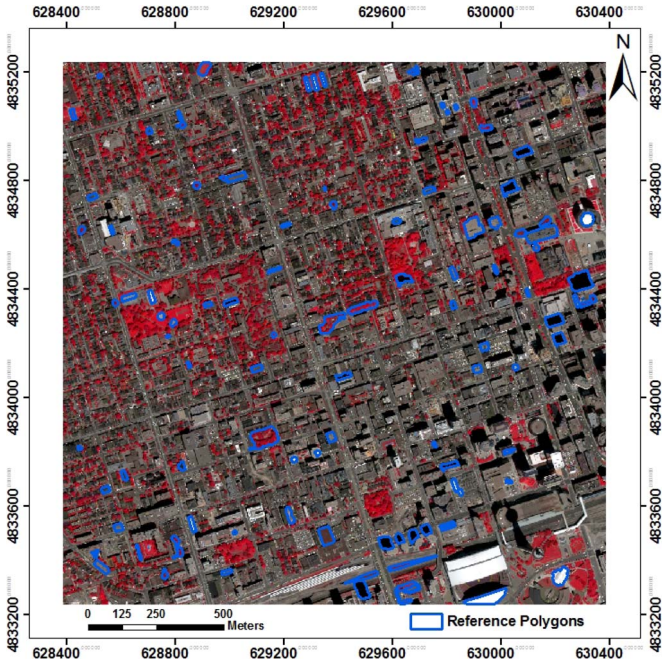

Fig. 1. False color composite of the WorldView-2 multispectral image with the near-infrared 1, red, and green bands displayed as red, green, and blue, respectively. The subset of the study area is under WGS84 UTM coordinate system.

reference polygon i, and J_i is the number of its corresponding segments. This modified equation has two advantages over previous methods: a candidate segment will be labeled as the corresponding segment of a reference polygon only when the overlapping area is over 50% of either the reference polygon or the candidate segment [16], [18], and the modified ED3 is a normalized index between zero and one, and a lower value of $\mathrm{ED3}_{\mathrm{Modified}}$ indicates a higher segmentation quality.

III. Experimental Results

A. Study Area and Experimental Image

The study area was located in the downtown of Greater Toronto Area, which is a metropolitan area in Ontario, Canada. It is a typical urban area, characterized by a complex mosaic of different land cover types, including street trees, grass, and many high-rise buildings. A WorldView-2 multispectral image was collected on June 2, 2011, containing eight spectral bands (i.e., coastal, blue, green, yellow, red, red edge, near-infrared 1, and near-infrared 2) with a resolution of 2 m. In this letter, a 2 $\times$ 2 km subset (see Fig. 1) was used to examine the performance of the proposed automated optimal scale parameterization.

B. Optimal Scale Parameterization

Multiresolution segmentation [5], a popular segmentation algorithm of the eCognition software (citation), was utilized to produce image segments using different scale parameters in this study. The segmentation was implemented at the scale parameter with a range from 20 to 120, whereas the other two parameters were fixed to the default values (i.e., color: 0.1; compactness: 0.5). The range of scale parameter was selected by taking into account the sizes of geo-objects in the experimental image. The global energy function E and the mean

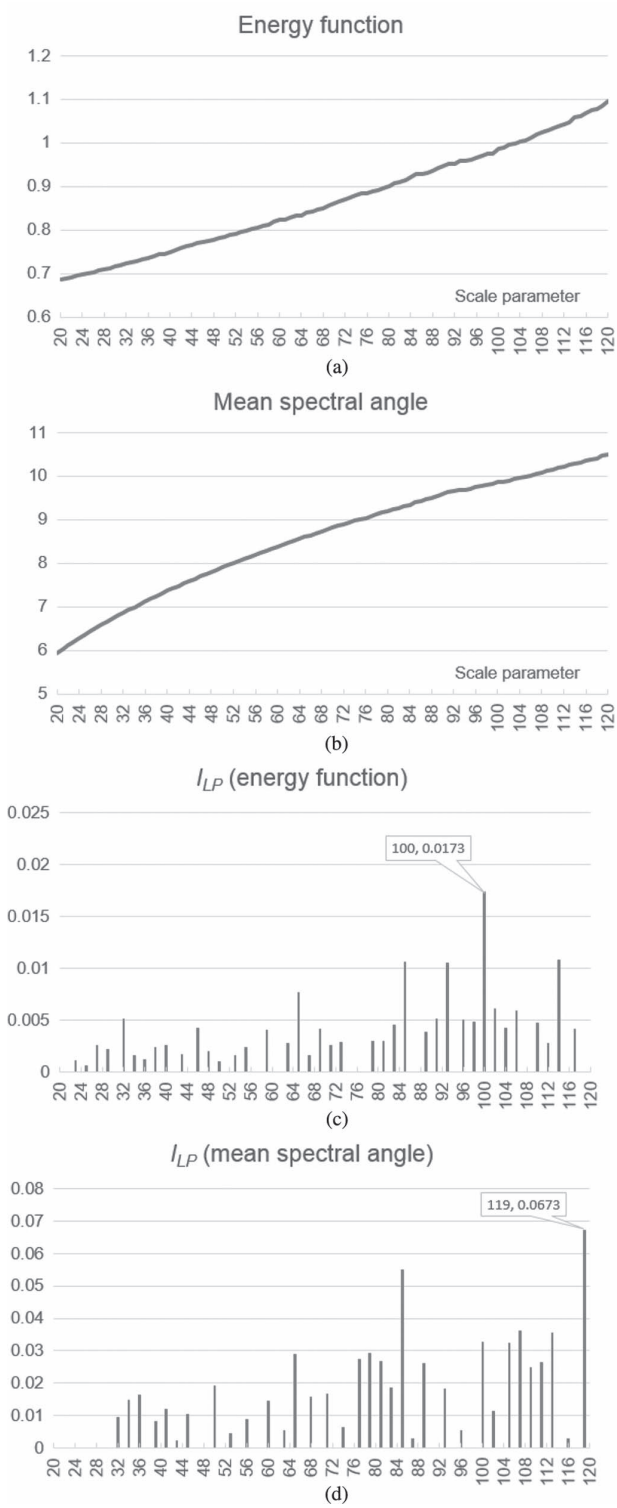

Fig. 2. (a) E, (b) Θ_{MEAN}, and the (c) and (d) corresponding I_{LP} values versus scale parameter.

spectral angle Θ_{MEAN} were calculated using (5) and (2), respectively. When the scale parameter increases from 20 to 120, we found that the E value increases from 0.69 to 1.09 [see Fig. 2(a)], whereas the Θ_{MEAN} value increases from 5.94 to 10.50 [see Fig. 2(b)]. Compared with the Θ_{MEAN} curve [see Fig. 2(b)], there are more flat terraces in the E curve [see Fig. 2(a)]. This demonstrates that the proposed energy function

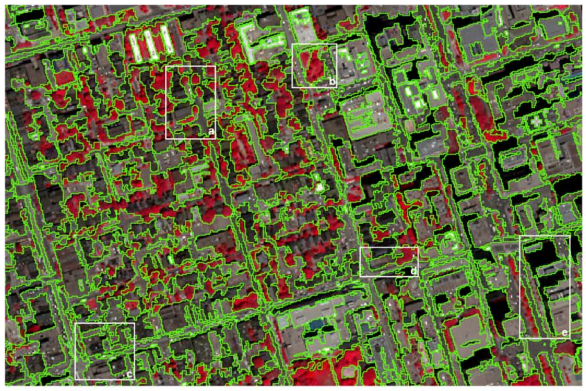

(a)

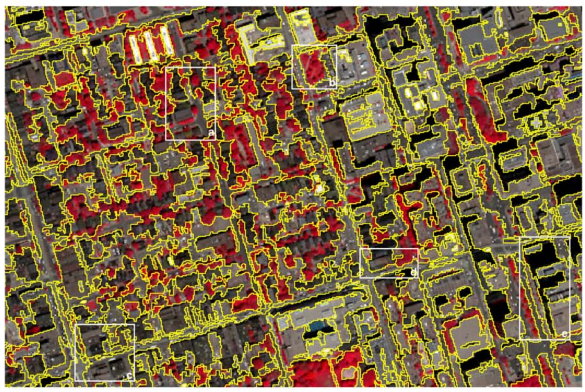

(b)

Fig. 3. Subset of the segmentation results at the scale parameter of (a) 100 and (b) 119, respectively.

E is able to produce more obvious LPs in the derivative curve and is more suitable for selecting the optimal scale parameter.

In order to further compare the two metrics, we calculated the values of I_{LP} for the scale parameters with the interval (Δl) of one. When Δl is equal to one, the largest value of I_{LP} for E is 0.0173 at the scale parameter of 100 [see Fig. 2(c)], whereas the largest value of I_{LP} for Θ_{MEAN} is 0.0673 at the scale parameter of 119 [see Fig. 2(d)]. In other words, the optimal scale parameters are determined to be 100 and 119 by the proposed energy function and mean spectral angle, respectively. Next, we will test which one is better through accuracy assessment.

C. Accuracy Assessment: Visual Interpretation and Quantitative Evaluation

To investigate and compare the performance of the proposed energy function E and the mean spectral angle Θ_{MEAN} for optimal segmentation scale parameterization, we manually digitized 100 reference polygons for different types and sizes of geo-objects, including impervious rooftops, vegetation, and shadows (blue polygons in Fig. 1).

For visual interpretation, a subset of the segmentation results of the preceding two optimized scale parameters is depicted in Fig. 3. For most of the vegetation and rooftop geo-objects, the segmentation results at the scale parameter identified by the proposed energy function (i.e., 100) outperform those at the scale parameter selected by the mean spectral angle (i.e., 119) because the segments at the scale parameter of 100 recognize the real geo-objects better [e.g., a, b, c, and d in Fig. 3(a)]. In contrast, the undersegmented vegetation [e.g., a and b in Fig. 3(b)] and rooftops [e.g., c and d in Fig. 3(b)] always exist at the scale parameter of 119. However, both of the scale parameters produce the same segmentation results for shaded geo-objects [see e in Fig. 3(a) and (b)]. This is probably due to their distinct spectral features and clear boundaries to the neighboring geo-objects.

TABLE I
DISCREPANCY MEASURE OF $\mathrm{ED3}_{\mathrm{Modified}}$ FOR SEGMENTATION EVALUATION AT THE SCALE PARAMETERS OF 100 AND 119

Scale parameter	100	119
$ED3_{Modified}$	0.2462	0.4251

Following the visual interpretation, the modified ED3 was calculated for the segmentation results at the scale parameters of 100 and 119. We can observe from Table I that the value of $\mathrm{ED3}_{\mathrm{Modified}}$ at the scale parameter of 100 (0.2462) is much lower than that at the scale parameter of 119 (0.4251). The modified ED3 provides results consistent with the visually interpreted ones because there are much more undersegmented geo-objects in the latter segmentation. In summary, both visual inspection and quantitative evaluation demonstrate that the LP-based method using the proposed energy function is more appropriate for optimal segmentation scale parameterization than using the mean spectral angle.

IV. DISCUSSION

In this letter, the proposed method optimized the segmentation result with a focus on the scale parameterization, the most important process for the characterization of the real geo-objects. It is worth noting that "scale parameterization" is not only referring to the optimization of the "scale" parameter, but a generalized definition of the parameter that controls the sizes of image segments. We have to keep in mind that this parameter is named differently in different segmentation algorithms. For instance, it is defined as the "scale" parameter by the multiresolution segmentation that was employed in this study, whereas it is named as the "threshold" parameter in the BerkeleyImageSeg software [19] and as the "scale level" parameter in the edge-based watershed algorithm [20] implemented in ENVI software. In the process of each segmentation algorithm, the sizes of segments are adjusted by increasing or decreasing the corresponding parameter. The proposed scale parameterization method is thus believed transferable when employing different algorithms to segment images for different types of landscapes (e.g., urban, forest, agricultural land, and wetland).

Regardless of visual inspection (i.e., trial and error), scale parameterization is categorized into the following: supervised (i.e., semiautomated) and unsupervised (i.e., automated) methods. The supervised method involves comparing image segments with reference geo-objects that were manually delineated by the user, whereas the unsupervised method involves scoring and ranking multiple segmentation results without the need for reference digitization. The supervised scale parameterization method has obvious advantage because it could provide satisfactory characterization of geo-objects from the perspective of human interpretation. However, it is too labor intensive and subjective for the user to manually digitize a large number of representative geo-objects. The proposed unsupervised method overcomes the preceding limitations and is able to make the scale parameterization more efficient and objective.

As aforementioned, segmentation results impact the follow-up image exploitation and interpretation, mainly geo-object recognition and image classification. It is quite understandable that higher segmentation quality would improve classification accuracy; however, the relationship between segmentation quality and classification accuracy is not always intuitive. As an example, oversegmentation would not negatively affect the accuracy of a classification map as long as the spectral features are distinct. In fact, oversegmentation may lead to a better classification because it helps classify smaller patches of land covers. In essence, however, the objective of image segmentation is to recognize real geo-objects rather than classification. When segmenting a forested image, for instance, we are first interested in the shapes and sizes of geo-objects (i.e., tree crowns), thereafter the species for each tree crown. In other words, image segmentation aims at geo-object recognition, thus should be independent upon classification.

V. Conclusion

In this letter, we have proposed a new energy function to simultaneously enhance the characteristics of intrasegment homogeneity and intersegment heterogeneity and incorporated the LP-based method for automated optimal scale parameterization. Additionally, a newly proposed discrepancy measure, ED3, was modified to quantitatively evaluate image segmentation. The effectiveness of the proposed method was examined by conducting an experiment with a multispectral WorldView-2 image of Toronto, Canada, and compared, visually and quantitatively, with the mean spectral angle that considered only intrasegment homogeneity. The results indicated that the proposed method provided a more suitable indicator for quantifying the fitness of matching segments with geo-objects.

By implementing the LP-based optimal scale parameterization, the advantages of the proposed energy function over the mean spectral angle were observed, because the energy function considered both intrasegment homogeneity and intersegment heterogeneity. Previous studies employed various metrics of intrasegment homogeneity for automated optimal scale parameterization, whereas this study demonstrated that the importance of intersegment heterogeneity should not be ignored. Studies [10] and [14] used the index of Moran's I for measuring intersegment heterogeneity; however, their parameterization principles were different from the LP-based method utilized in this letter. Compared with Moran's I, the gradient measure improved the process mainly in the following two aspects. First, the proposed gradient measure made full use of multiple spectral bands to measure intersegment heterogeneity, whereas Moran's I was a single-band measure. Meanwhile, it required extra preprocessing to select a suitable spectral band for analysis with the Moran's I method. Second, Moran's I computed intersegment heterogeneity not only for neighboring segments but also for those within a specific distance, leading to a more time consuming process. In the future, it would be beneficial to explore the relationship between the LP magnitude and the segmentation accuracy with more experimental images of diverse landscapes.

Acknowledgment

The authors would like to thank the Department of Geography of the University of Toronto Mississauga for funding from the Graduate Expansion Fund to cover the overlength page charges and the anonymous reviewers for providing their valuable comments and suggestions.

References

[1] D. Comaniciu and P. Meer, "Mean shift: A robust approach toward feature space analysis," *IEEE Trans. Pattern Anal. Mach. Intell.*, vol. 24, no. 5, pp. 603–619, May 2002.

[2] C. M. Christoudias, B. Georgescu, and P. Meer, "Synergism in low level vision," in *Proc. 16th Int. Conf. Pattern Recog.*, Quebec City, QC, Canada, 2002, vol. 4, pp. 150–155.

[3] J. Michel, D. Youssefi, and M. Grizonnet, "Stable mean-shift algorithm and its application to the segmentation of arbitrarily large remote sensing images," *IEEE Trans. Geosci. Remote Sens.*, vol. 53, no. 2, pp. 952–964, Feb. 2014.

[4] M. Baatz and A. Schäpe, "Multiresolution segmentation: An optimization approach for high quality multi-scale image segmentation," in *Proc. 12th Angewandte Geographische Informationsverarbeitung*, 2000, pp. 12–23.

[5] U. C. Benz, P. Hofmann, G. Willhauck, I. Lingenfelder, and M. Heynen, "Multi-resolution, object-oriented fuzzy analysis of remote sensing data for GIS-ready information," *ISPRS J. Photogramm. Remote Sens.*, vol. 58, no. 3/4, pp. 239–258, Jan. 2004.

[6] L. Vincent and P. Soille, "Watersheds in digital spaces: An efficient algorithm based on immersion simulations," *IEEE Trans. Pattern Anal. Mach. Intell.*, vol. 13, no. 6, pp. 583–598, Jun. 1991.

[7] P. Li, J. Guo, B. Song, and X. Xiao, "A multilevel hierarchical image segmentation method for urban impervious surface mapping using very high resolution imagery," *IEEE J. Sel. Topics Appl. Earth Obs. Remote Sens.*, vol. 4, no. 1, pp. 103–116, Mar. 2011.

[8] D. Li, G. Zhang, Z. Wu, and L. Yi, "An edge embedded marker-based watershed algorithm for high spatial resolution remote sensing image segmentation," *IEEE Trans. Image Process.*, vol. 19, no. 10, pp. 2781–2787, Oct. 2010.

[9] J. Yang, Y. He, and J. Caspersen, "A multi-band watershed segmentation method for individual tree crown delineation from high resolution multispectral aerial image," in *Proc. IEEE IGARSS*, Quebec City, QC, Canada, 2014, pp. 1588–1591.

[10] G. Espindola, G. Câmara, I. Reis, L. Bins, and A. Monteiro, "Parameter selection for region-growing image segmentation algorithms using spatial autocorrelation," *Int. J. Remote Sens.*, vol. 27, no. 14, pp. 3035–3040, Jul. 2006.

[11] M. Kim, M. Madden, and T. Warner, "Estimation of optimal image object size for the segmentation of forest stands with multispectral IKONOS imagery," in *Object-Based Image Analysis. Spatial Concepts for Knowledge-Driven Remote Sensing Applications*, T. Blaschke, S. Lang, and G. J. Hay, Eds. Berlin, Germany: Springer-Verlag, 2008, pp. 291–307.

[12] M. Kim, M. Madden, and T. A. Warner, "Forest type mapping using object-specific texture measures from multispectral IKONOS imagery: Segmentation quality and image classification issues," *Photogramm. Eng. Remote Sens.*, vol. 75, no. 7, pp. 819–829, Jul. 2009.

[13] L. Draguţ, D. Tiede, and S. R. Levick, "ESP: A tool to estimate scale parameter for multiresolution image segmentation of remotely sensed data," *Int. J. Geograph. Inf. Sci.*, vol. 24, no. 6, pp. 859–871, Apr. 2010.

[14] B. Johnson and Z. Xie, "Unsupervised image segmentation evaluation and refinement using a multi-scale approach," *ISPRS J. Photogramm. Remote Sens.*, vol. 66, no. 4, pp. 473–483, Jul. 2011.

[15] L. Draguţ, O. Csillik, C. Eisank, and D. Tiede, "Automated parameterisation for multi-scale image segmentation on multiple layers," *ISPRS J. Photogramm. Remote Sens.*, vol. 88, pp. 119–127, Feb. 2014.

[16] J. Yang, P. Li, and Y. He, "A multi-band approach to unsupervised scale parameter selection for multi-scale image segmentation," *ISPRS J. Photogramm. Remote Sens.*, vol. 94, pp. 13–24, Aug. 2014.

[17] A. Carleer, O. Debeir, and E. Wolff, "Assessment of very high spatial resolution satellite image segmentations," *Photogramm. Eng. Remote Sens.*, vol. 71, no. 11, pp. 1285–1294, Nov. 2005.

[18] Y. Liu *et al.*, "Discrepancy measures for selecting optimal combination of parameter values in object-based image analysis," *ISPRS J. Photogramm. Remote Sens.*, vol. 68, pp. 144–156, Mar. 2012.

[19] Berkeley Image Segmentation; *Berkeley Environmental Technology International*, LLC.: Long 339 Beach, CA, USA. [Online]. Available: http://www.imageseg.com/

[20] X. Jin, "Segmentation-based image processing system" U.S. Patent 8 260 048, filed Nov. 14, 2007, and issued Sep. 4, 2012.